Holographic Gratings in Azobenzene Side-Chain Polymethacrylates

Luisa Andruzzi, Angelina Altomare, Francesco Ciardelli, and Roberto Solaro

Department of Chemistry and Industrial Chemistry, University of Pisa, via Risorgimento 35, 56126 Pisa, Italy

Søren Hvilsted*

Condensed Matter Physics and Chemistry Department, Risø National Laboratory, DK-4000 Roskilde, Denmark

P. S. Ramanujam

Optics and Fluid Dynamics Department, Risø National Laboratory, DK-4000 Roskilde, Denmark

Received February 4, 1998; Revised Manuscript Received October 19, 1998

ABSTRACT: Optical storage properties of thin unoriented liquid crystalline and amorphous side-chain azobenzene polymethacrylate films are examined by polarization holographic measurements. The investigated materials are free radical copolymers derived from two photochromic monomers, 6-(4-oxy-4′-cyanoazobenzene)hex-1-yl methacrylate and 8-(4-oxy-4′-cyanoazobenzene)oct-1-yl methacrylate, and a nonphotochromic optically active comonomer, (−)-menthyl methacrylate. The thermal behavior and phase transitions of the polymers have been investigated in detail through differential scanning calorimetry and polarizing optical microscopy. Atomic force microscopy investigations have been carried out on the polarization holographic gratings recorded in the polymethacrylate films. A surface relief grating has been found to appear in all films after irradiation. The copolymers with 50−75% dye content exhibit the largest surface relief. The stored information seems to be stable up to approximately 70 °C, except in the case of polymers with low dye content.

1. Introduction

Polymers with pendant azobenzene moieties in the side chains are potentially useful as materials for optical information storage.[1−5] The methacrylate systems in particular have been studied in great detail by Natansohn's group.[6−8] The attractive features of these systems are the high birefringence obtainable due to polarized laser beam irradiation and the erasability of the induced anisotropy on irradiation with circularly polarized light. Natansohn et al.[9] have also investigated the interaction between the side chains when the polymethacrylate contained both azobenzene and polar or nonpolar side chains. It was shown that a higher birefringence is obtained when the side chains are polar due to a cooperative motion of the azobenzenes. We have previously investigated the effect of the introduction of an optically active comonomer in a methacrylate polymer containing azo groups,[10−12] aimed in principle to give rise to a structural noncentrosymmetry to improve the nonlinear optical properties.[13] Besides the investigation of the nonlinear optical properties in the solid state such as second harmonic generation, it is also of interest to investigate the correlations between the chirooptical properties and the eventual photoinduced changes of the secondary structure of the polymers.[14−16]

All azobenzene-containing polymers exhibit a surface relief grating in addition to a birefringent grating,[17−21] when irradiated with two polarized light beams. The magnitude of the surface relief is different depending on the polymer system. One of the aims of the current investigation is to examine the surface relief introduced in the material as a function of the concentration of the azo dye.

* To whom correspondence should be addressed. e-mail s.hvilsted@risoe.dk.

After a brief introduction to the preparation and characterization of the polymers, we discuss differential scanning calorimetric (DSC) and polarizing optical microscopic (POM) characterization of two series of methacrylic polymers based on the mesogenic photochromic monomers, 6-(4-oxy-4′-cyanoazobenzene)hex-1-yl methacrylate (**MC6**) and 8-(4-oxy-4′-cyanoazobenzene)-oct-1-yl methacrylate (**MC8**), and an optically active comonomer, (−)-menthyl methacrylate (**MnMA**). Optical storage in thin films of these polymers is investigated through a polarization holographic technique, and atomic force microscopy investigations have been performed to give more details of the storage mechanism.

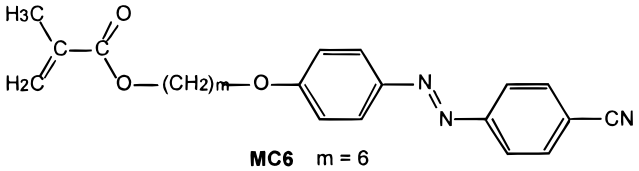

MC6 m = 6
MC8 m = 8

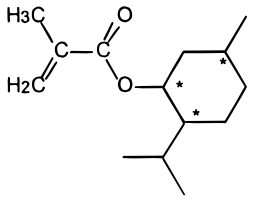

MnMA

2. Experimental Section

Preparation of the Polymers. The polymers were synthesized by free radical homo- and copolymerization of the photochromic monomers 6-(4-oxy-4′-cyanoazo-benzene)hex-1-yl methacrylate (**MC6**) and 8-(4-oxy-4′-cyanoazobenzene)oct-

10.1021/ma980160j CCC: $18.00 © 1999 American Chemical Society
Published on Web 01/05/1999

Table 1. Thermal Data of Homopolymers PC6 and PC8, Their Copolymers with (−)-Menthyl Methacrylate (PC*m*Mn(*x*)), and PMnMA

polymer	MC*m*[a] (mol %)	T_g (°C)	T_{SA} (°C)	T_N (°C)	T_i (°C)	ΔH_i (kJ/mol)
PC6	100	60	163		168	1.84
PC6Mn(1)	92	57		123	125	1.37
PC6Mn(2)	76	69			92	0.24
PC6Mn(3)	51	80				
PC6Mn(4)	27	104				
PC6Mn(5)	7	131				
PC8	100	35	158		162	2.68
PC8Mn(1)	95	35	138		141	2.33
PC8Mn(2)	79	58			99	1.09
PC8Mn(3)	51	65				
PC8Mn(4)	30	90				
PC8Mn(5)	7	124				
PMnMA		147				

[a] Mole percent azo-containing monomer as determined by ^{1}H NMR.

1-yl methacrylate (**MC8**) with (−)-menthyl methacrylate (**MnMA**), as reported elsewhere.[22]

The copolymers of azo methacrylates with (−)-menthyl methacrylate are denoted **PC*m*Mn(*x*)** where $m = 6$ or 8 and $x = 1, 2, 3, 4$, or 5 for different lengths of the polymethylene spacer and different dye mole contents, respectively, as reported in Table 1. The homopolymers are denoted **PC6** and **PC8**, corresponding to the hexamethylene and octamethylene spacers, respectively.

The size exclusion chromatography (SEC) analysis revealed the polymethacrylates number-averaged molecular mass distribution to be of Gaussian shape and the number-average molecular masses to range among 10 000 and 30 000, with polydispersities 1.7−2.7.

Preparation of Thin Films. For polarizing optical microscopic investigations, thin polymer films were cast from a chloroform solution. The films are typically 4−10 μm thick. The films were dried under vacuum at temperatures ranging between 60 and 100 °C. For holographic measurements, thin films were prepared by dissolving approximately 40 mg of the polymer in 150 μL of tetrahydrofuran and 30 mg of the material in 200 μL of hexafluoro-2-propanol respectively for the **PC6** and **PC8** series of polymers and spin-coating them at 1200 rpm on to glass substrates, typically 20 mm in diameter. The films were then dried in a vacuum oven at room temperature for 3 h. The films were not preoriented in any fashion.

Differential Scanning Calorimetry (DSC). DSC experiments were performed on a Mettler TA-400 instrument equipped with baseline calibration systems and computerized data elaboration systems. The experiments were run in the temperature range −30 to 200 °C on 5−10 mg polymeric samples under nitrogen atmosphere, utilizing either heating or cooling rates ranging from 2 to 15 °C min^{-1}.

Polarizing Optical Microscopy (POM). The POM observations were made with a Reichert Polyvar polarizing microscope equipped with a Mettler FP-52 hot stage controlled by a Mettler FP-5 unit. The heating and cooling cycles were performed at the rate of 10 °C min^{-1} up to a temperature 10 °C lower than the isotropization point and at the rate 0.2−0.3 °C min^{-1} up to the formation of liquid.

Polarization Holography. Figure 1 shows a typical setup for two-beam polarization holography. An argon ion laser (Innova 90-6) at 488 nm is used as the source. The argon ion laser is divided into two by means of a polarization beam splitter (PBS). The ratio of the intensities of the two beams can be adjusted by rotating the half-wave plate (HWP). The two beams are overlapped in the film through the adjustments of mirrors, M. Before falling on the film, the beams pass through suitably oriented quarter-wave plates (QWP) in order to convert the beams to orthogonally circularly polarized beams. A He−Ne laser with a power of 4 mW is used to monitor the first-order diffraction efficiency. A quarter-wave plate converts the linearly polarized beam from the He−Ne laser to a circularly polarized beam. The laser power controller (LPC) is used to select a given laser power. The polymer film is mounted on a Peltier element which enables the temperature of the film to be controlled.

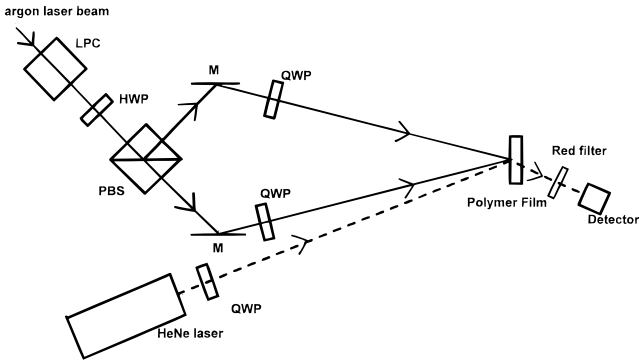

Figure 1. An experimental setup to record polarization holographic gratings: HWP, a half-wave plate; LPC, laser power controller; M, mirrors; PBS, polarizing beam splitter; QWP, quarter-wave plates. The film is mounted on a Peltier element facilitating heating and cooling of the film.

Atomic Force Microscopy (AFM). The AFM investigations of the grating structures in polymethacrylate films recorded using polarization holography were carried out with a Topometrix Explorer atomic force microscope at the laser-irradiated spot of the film. Typically an area of 20 μm × 20 μm was scanned.

Film Thickness Measurements. The film thickness measurements have been performed with a Dektak 3030 surface profile measuring system.

3. Results and Discussion

Differential Scanning Calorimetry (DSC). The results of the DSC investigations on the polymers are summarized in Table 1. The table reveals the presence of a glass transition in all the polymers. In the case of polymers characterized by azo-dye content higher than 75%, first-order transitions are also observed. These measurements show the monophase nature of the polymethacrylates. Thermal treatments of the samples (slow cooling from the isotropization temperature, T_i, to room temperature and annealing for several hours at T_i) did not bring about any changes in the thermal traces. The T_g of the photochromic homopolymers is seen to decrease from 60 to 35 °C while the length of the polymethylene spacer increases from 6 to 8. This kind of behavior, as reported in the literature,[23] can be attributed either to the increasing decoupling of the side chains from the main chain or to the plasticizing effect of the polymethylene spacer chain.

The first-order transition temperature relative to the two homopolymers **PC6** and **PC8** ranges from 162 to 168 °C and the corresponding enthalpy values range from 1.8 to 2.7 kJ mol^{-1}. These are typical values for the isotropization processes of smectic A phases.[23]

The copolymers characterized by azo-dye content higher than 75% also show a similar behavior, and in particular the values of T_i and ΔH_i decrease with increasing content of **MnMA** units. The thermal traces of copolymers characterized by an azo-dye content lower than 75% only show a T_g. The T_g increases with increasing content of (−)-menthyl methacrylate, possibly due to an increase of the chain stiffness.

Polarizing Optical Microscopy (POM). Polymer films were subjected to different thermal treatments with the primary aim to promote the formation of

mesophases and to allow the identification of optical textures typical of liquid crystalline (LC) phases. The films of polymers containing more than 75% azo units are characterized by a single LC phase transition corresponding to the isotropization of the polymers. In every case POM observations result in perfectly reversible cycles in either heating or cooling. This points to the presence of an enantiotropic transition.

It should be noted that all the observed samples are characterized at room temperature by a rather ill-defined texture, lacking in distinctive optical features. For poly(methacrylate)s **PC6**, **PC6Mn(1)**, **PC8**, and **PC8Mn(1)** it was possible, after the first heating−cooling cycle to identify optical features typical of smectic A (S_A) (**PC6**, **PC8**, and **PC8Mn(1)**) and nematic phase (**PC6Mn(1)**).

Photomicrographs showing optical texture changes upon cooling at 0.2 °C min^{-1} from the isotropic state to room temperature films of **PC6** and **PC6Mn(1)** are shown in Figure 2. Batonnet features typical of a pretransitional state of a S_A phase for **PC6** are depicted in Figure 2a. An optical texture consisting of irregularly distributed focal conic features typical of the S_A phase is shown in Figure 2b. Finally, Figure 2c shows an optical texture consisting of schlieren features typical of a nematic phase for **PC6Mn(1)**.

On the other hand, for polymers **PC6Mn(2)** and **PC8Mn(2)**, thermal treatments (slow cooling at 0.2 °C min^{-1} from the isotropic state to room temperature or annealing for 5 h at a temperature close to the clearing point) did not promote a defined textural pattern. Therefore, it was not possible to make a definite assignment of the observed texture.

The POM investigations on the monomers **MC6** and **MC8** revealed the direct melting to the isotropic state at the temperatures of 90 and 92 °C, respectively, without exhibiting any mesophases. The results show that the mesogenic tendency of the azobenzene units is remarkably increased when they are linked to a macromolecular chain due to the cooperative interactions between the side chains. This brings about a rather extended mesophase ($T_i - T_g > 80$ °C) in the copolymers characterized by a high thermal stability.

Copolymerization of photochromic monomers with **MnMA** increases the average distance between neighboring chromophores. This reduces the stability and the extent of the structural order of the mesophase. Only a relatively low content (<25%) of **MnMA** counits can be tolerated in the copolymers without completely losing the LC phase.

POM investigations have not revealed the formation of chiral LC phases in any of the examined copolymers despite the presence of optically active **MnMA** counits. This incapability of the copolymers to give rise to chiral LC phases could be due to the flexibility of the hydrocarbon spacers and to the relatively long distance separating the mesogens from the chiral units. This makes the mutual interactions between the side chains less probable.

Holographic Measurements. *Time-Dependent Measurements of the Diffraction Efficiency.* As mentioned earlier, the experimental system allows measurements to be made at different laser intensities and film temperatures. During the first 5 s of measurements, only the HeNe laser is on; this is to observe the presence of any residual diffraction grating in the film. The argon ion laser is switched on after 5 s and switched off after 60 s, and the diffraction efficiency is followed on for a period of 60 s more in order to observe any decay of the diffraction efficiency. All the films display a permanent grating structure after the argon ion laser is switched

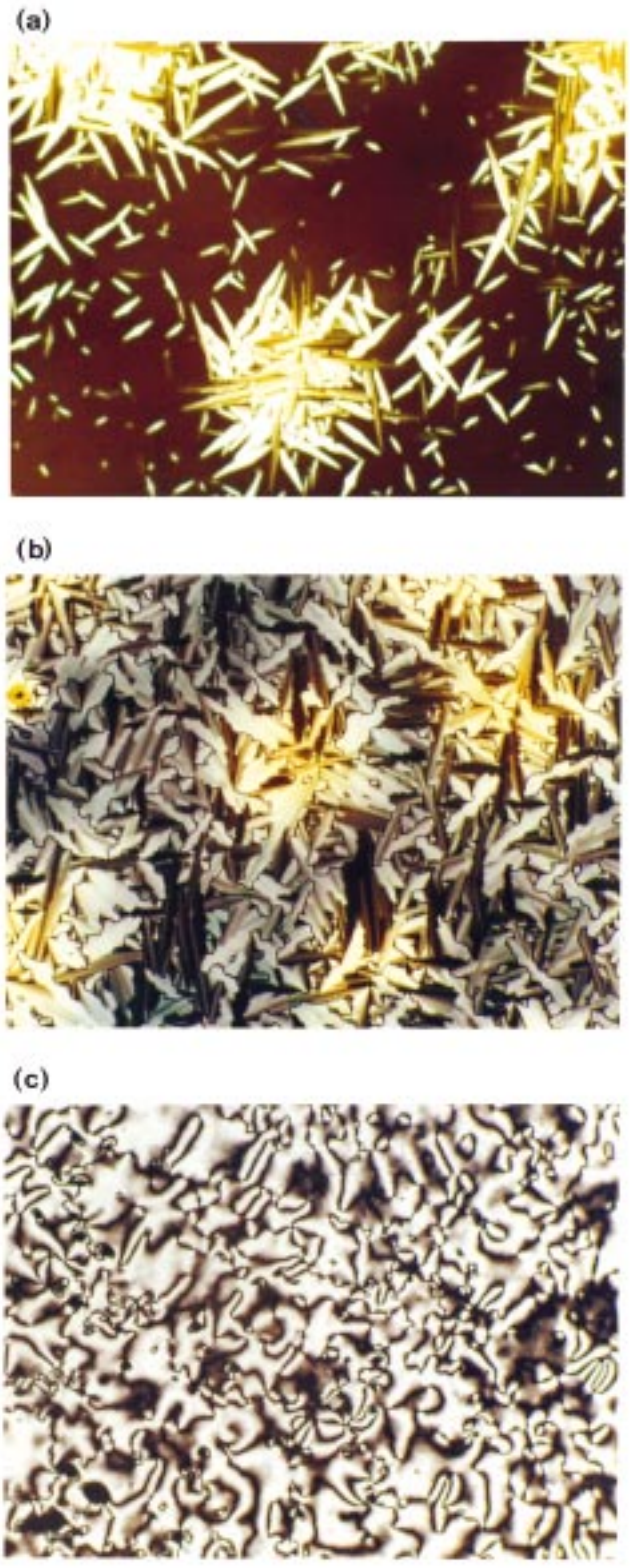

Figure 2. Photomicrographs showing optical texture changes, upon cooling from the isotropic state to room temperature at 0.2 °C min^{-1} of **PC6** and **PC6Mn(1)** films: (a) batonnet features forming at 164 °C in **PC6** film, (b) focal conic textures of S_A phase forming at 163 °C in **PC6** film, (c) schlieren textures of a nematic phase forming at 123 °C in **PC6Mn(1)** film. Crossed polarizers, magnification ×320.

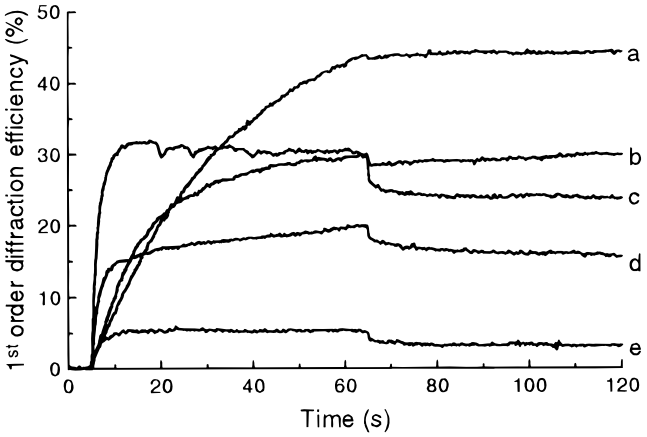

Figure 3. First-order diffraction efficiency in (a) **PC6** homopolymer and **PC6Mn(*x*)** polymers: (b) $x = 1$, (c) $x = 2$, (d) $x = 3$, and (e) $x = 4$, as a function of time at 25 °C. The argon laser is switched on after 5 s and switched off after 60 s; the intensity of the laser beam is 1.5 W cm^{-2}. The diffraction efficiency is measured for a further 60 s.

Table 2. Diffraction Efficiencies of PC6 Polymers

		without slide on top		with slide on top	
polymer	**MC6** (mol %)	max diffr eff (%)	T_e[a] (°C)	max diffr eff (%)	T_e[a] (°C)
PC6	100	44	65	54	59
PC6Mn(1)	92	31	67	39	61
PC6Mn(2)	76	24	49	28	40
PC6Mn(3)	51	15	60	10	49
PC6Mn(4)	27	4	58	5	40

[a] Erasure temperature defined here as that temperature at which the maximum diffraction efficiency has decreased to 90% of the maximum value.

Table 3. Diffraction Efficiencies of PC8 Polymers

polymer	**MC8** (mol %)	max diffr eff (%)	T_e[a] (°C)
PC8	100	34	66
PC8Mn(1)	95	31	59
PC8Mn(2)	79	29	50
PC8Mn(3)	51	15	56
PC8Mn(4)	30	4	57

[a] Erasure temperature defined here as that temperature at which the maximum diffraction efficiency has decreased to 90% of the maximum value.

off, even though some of the films show an initial small decay.

Figure 3 shows the first-order diffraction efficiency of the polymethacrylates with hexamethylene spacers as a function of time for an incident intensity of the argon ion laser of 1.5 W/cm^2. The decay of the diffraction efficiency after the laser is switched off might be due to a thermal effect; i.e., the film cools and the chromophores relax to a certain extent with a consequent decreasing in diffraction efficiency.[24]

For both the series of polymers it can be pointed out that the higher the content of dye in the polymer, the higher the value of the achieved maximum diffraction efficiency (Tables 2 and 3).

The polymethacrylates with the hexamethylene spacer seem to possess a shorter rise time and a higher value of diffraction efficiency with respect to the polymethacrylates with the octamethylene spacer.

Temperature-Dependent Measurements of the Diffraction Efficiency. Typical erasure temperatures for the two series of polymers are also shown in Tables 2 and 3. Figure 4 shows the temperature dependence of the

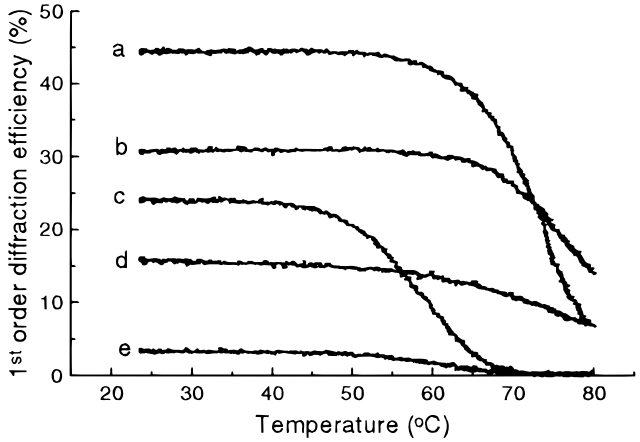

Figure 4. First-order diffraction efficiency in (a) **PC6** homopolymer and **PC6Mn(*x*)** polymers: (b) $x = 1$, (c) $x = 2$, (d) $x = 3$, and (e) $x = 4$, as a function of temperature. The gratings were recorded at a temperature of 25 °C; heating rate is 1 °C s^{-1}.

diffraction efficiency for **MC6**-containing polymers.

In general, for **MC6** polymers erasure is an easier process than for the ones belonging to **MC8** series.

The **PC*m*Mn(2)** ($m = 6$ or 8) films have lower erasure temperatures than either **PC*m*Mn(1)** or **PC*m*Mn(3)**. As far as **PC*m***, **PC*m*Mn(1)**, and **PC*m*Mn(2)** samples are concerned, the possibility of erasure might depend on structural factors. The erasure temperature decreases in general going from the homopolymer to the 75% copolymer with the decreasing degree of structural order. The LC order decreases passing from a smectic A phase in **PC6** to a nematic phase in **PC6Mn(1)** to a fine grained texture in **PC6Mn(2)** and from a highly ordered smectic A phase in **PC8** to a less ordered smectic A phase in **PC8Mn(1)** to a fine grained texture in **PC8Mn(2)**. In the LC samples the structural order might be the factor stabilizing the photoinduced optical anisotropy; hence, the erasure process may not depend on the T_g. On the other hand, **PC*m*Mn(3)** and **PC*m*Mn(4)** are amorphous polymers where the erasure process may be dependent on the T_g. As this value is reasonably high and higher than those of the high azo-dye content polymers, one can expect to have a higher T_e despite the lower azo-dye content. Examination of the films with an atomic force microscope (described in detail in the following) after recording the grating showed the presence of a surface relief. The surface relief can be erased by heating the films up to a temperature of 130 °C in all cases, which is well above the glass transition temperature. Films with the surface relief can as easily be dissolved in common solvents such as THF as unexposed films. This indicates that cross-linking may not be the reason for the stability of the surface relief. We believe that an increased order created in the films due to the alignment of the chromophores may be responsible for the stability of the surface relief.

The importance of thermal processes in the formation of the surface relief cannot be neglected. It has been pointed out before[25] that a temperature increase of several degrees locally can be induced due to the laser irradiation. This can plasticize the surface, enabling the formation of a surface relief.

Despite the large differences in the glass transition temperatures between the **PC6** and the **PC8** series, the erasure temperatures do not vary drastically for the homologues. The length of the side chain does not seem to play a prominent role in the erasure process.

Contribution to the Diffraction Efficiency from Anisotropy and Surface Relief. We have shown[26] that the contributions of anisotropy and surface relief to the diffraction efficiency can be estimated through a measurement of the first-order diffraction efficiency as follows. The grating is written with two orthogonally polarized beams and is probed using a linearly polarized HeNe laser beam. The first-order diffracted beam is split into a horizontal (h) and a vertical (v) component using a Wollaston prism. Using Jones calculus, the intensities of the two beams after the Wollaston prism are

$$I_{vv} = |a + be^{i\delta_0}|^2 = a^2 + b^2 + 2ab\cos\delta_0$$

and

$$I_{vh} = a^2$$

Here the first index, v, refers to the vertical polarization of the probe beam, and the second indices, v or h, refer to the vertical and horizontal component of the diffracted wave.

For horizontal polarization of the probe beam we obtain

$$I_{hv} = a^2$$

and

$$I_{hh} = |-a + be^{i\delta_0}|^2 = a^2 + b^2 - 2ab\cos\delta_0$$

Thus, by measuring the intensities I_{vv}, I_{vh}, I_{hh}, and I_{hv}, we can find a, b, and δ_0. In the above equations, $a = \sin(\Delta\varphi)/2$ and $b = \cos(\Delta\varphi)\, J_1(\Delta\psi)$. Here, $\Delta\varphi = \pi(\delta n)d/\lambda$ is the anisotropic phase shift due to the induced birefringence δn, d is the film thickness, and λ is the wavelength. $\Delta\psi = \pi(\Delta n)(\Delta d)/\lambda$, Δn is the difference between the refractive index of the polyester and air, and $(2\Delta d)$ is the relief height. $J_1(\Delta\Psi)$ is the first-order Bessel function of the first kind in $\Delta\psi$. δ_0 is the displacement between the anisotropic and topographic gratings. The values of $\Delta\varphi$ and $\Delta\psi$ can thus be determined.

The normalized intensity curves obtained for the case of **PC6Mn(1)** are shown in Figure 5a for an intensity of 250 mW/cm^2 at a wavelength of 488 nm. Figure 6 shows the phase difference due to anisotropy, $\Delta\varphi$, and due to the surface relief, $\Delta\psi$, as a function of time. From Figure 5a it is seen that for longer exposure times (fluence) $I_{hh} > I_{vv}$. This means that there is a displacement of π between the anisotropy and surface relief as defined. In other words, the trenches of the surface relief correspond to horizontal polarization of light. As shown in the expansion in Figure 5b, for less than 30 s of exposure, however, $I_{vv} > I_{hh}$, which leads to the conclusion that the peaks of the surface relief correspond to the horizontal polarization. This is also clearly reflected in Figure 6. Thus as the fluence increases, the displacement of the surface relief changes. This has been observed for other **PC6** films as well. At higher intensity, I_{vh} and I_{hv} are both much smaller than I_{vv} and I_{hh}, indicating that surface relief is the dominating factor from the start.

Atomic Force Microscopic (AFM) Investigations. The films were examined with an atomic force microscope after recording a grating. The gratings were recorded under similar conditions to those described above. It was found that all the examined samples exhibit a surface relief at the expected optical spatial frequency.

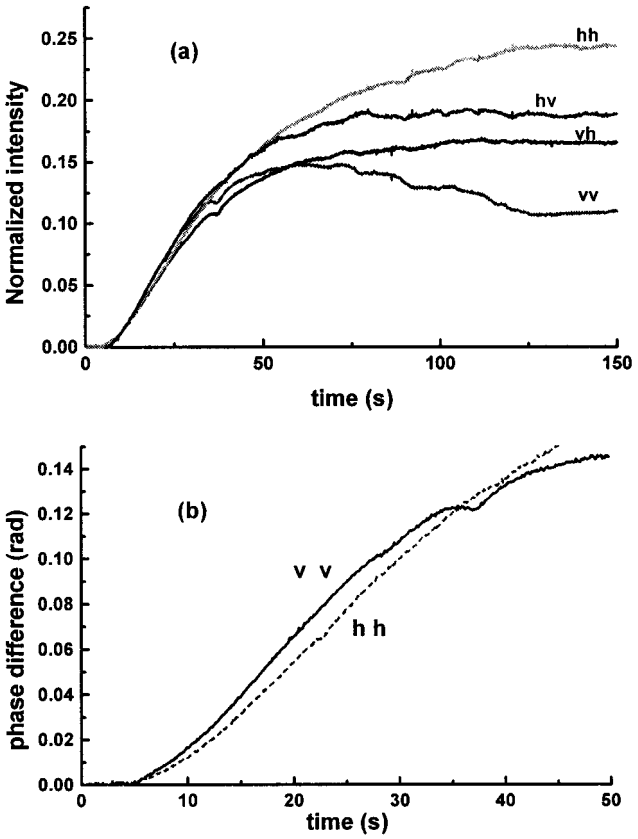

Figure 5. (a) Normalized intensity curves, I_{vv} (vv), I_{vh} (vh), I_{hv} (hv), and I_{hh} (hh), in **PC6Mn(1)** as a function of time for a laser intensity of 250 mW/cm^2. (b) Expansion of I_{vv} (vv) and I_{hh} (hh) during the first 50 s.

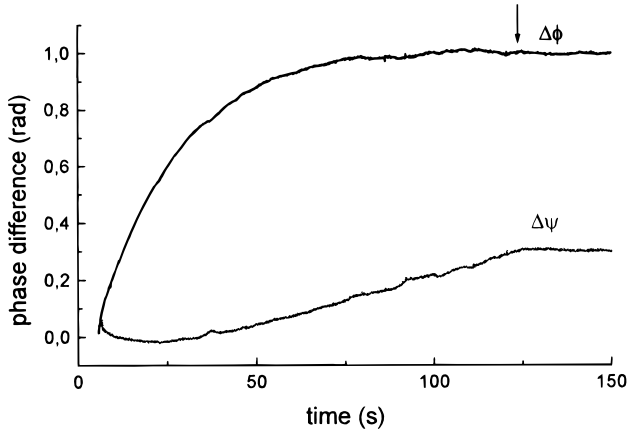

Figure 6. Calculated values of the phase difference due to anisotropy, $\Delta\varphi$, and due to surface relief, $\Delta\psi$, obtained from Figure 5. The arrow denotes the point where the laser is switched off.

In Table 4, the thickness of the films and the maximum height of the surface relief obtained in the **PC6** and **PC8** polymers are reported. A direct comparison between the two must be done with caution, since the films in this case have been prepared with different solvents, leading to different thicknesses.

Figure 7 shows an atomic force microscope 20 μm × 20 μm scan of the irradiated area of **PC6Mn(1)**. The homopolymers (**PC6** and **PC8**) show a small surface relief, comparable by the way to the one with the lowest

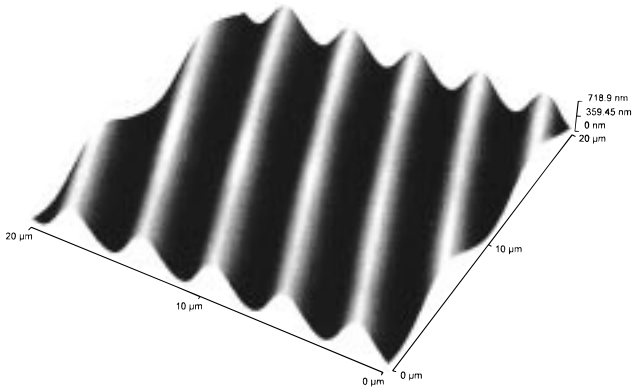

Figure 7. AFM scan of a polarization diffraction grating recorded in a film of **PC6Mn(1)**. The scanned area is 20 μm × 20 μm. The maximum surface relief is shown along the vertical axis.

Table 4. Surface Relief Heights of Thin Films of the PC6 and PC8 Polymers

polymer	**MC*m*** (mol %)	height (nm)	film thickness (μm)
PC6	100	200	4.5
PC6Mn(1)	92	780	4.8
PC6Mn(2)	76	1340	5.0
PC6Mn(3)	51	740	4.3
PC6Mn(4)	27	215	5.1
PC8	100	90	1.3
PC8Mn(1)	95	80	1.5
PC8Mn(2)	79	900	1.3
PC8Mn(3)	51	475	1.4
PC8Mn(4)	30		1.7

azo-dye content (approximately 25%) copolymers (**PC6Mn-(4)**). It must be mentioned that it has not been possible to measure the surface relief in **PC8Mn(4)**.

Surface relief in azobenzene-containing polymers has been observed before.[17−20] At the moment, no concrete theory exists to explain the presence of the surface relief. Current published explanations are based on thermal effects[17] or pressure gradients due to the free-volume requirements during trans−cis isomerization of the azobenzene.[20] However, these fail to explain the polarization dependence of the observed surface relief in azobenzene polyesters.[21] While free-volume requirements when the molecule undergoes a trans−cis isomerization may be responsible for the initiation of topographic features, it is obvious that more than one mechanism is important in the formation of the final surface relief. We[27] have proposed that a Maier−Saupe potential for the interaction between the dipoles may be responsible for the surface relief in side-chain liquid crystalline polyesters. However, this does not explain all the observed features in the present case. It may be necessary to consider long-range electrostatic interactions between the dipoles as well. It is clear from a study of azobenzene dendrimers[28] that molecular arrangement is an important parameter. More experimental evidence is needed for a complete understanding of the mechanism for the formation of the surface relief.

Intuitively, one might expect the homopolymers to exhibit the largest relief as the concentration of azobenzene chromophores is largest as this might promote a greater interaction between the chromophores. However, it is noteworthy that **PC6Mn(2)** and **PC8Mn(2)** copolymers containing approximately 75% azo dye are characterized by the highest surface relief. Another interesting feature is that even though **PC*m*Mn(2)** shows the highest surface relief, the diffraction efficiency is smaller than in homopolymers. This is due to the fact that the surface relief is a porous structure with a smaller density. Thus, the change in the refractive index between "peaks" and "valleys" is not large. Similar observations have been made in an oligopeptide,[29] where a surface relief approximately 10 times the pristine film thickness was obtained on irradiation with a single off-axis p-polarized laser beam.

We have also made diffraction efficiency measurements on **PC6** series films with a glass cover glued on top of the polymer film. This prevents the formation of a surface relief and hence affects the temperature stability of the recorded gratings. As seen in Table 2, these gratings are erased at lower temperatures compared to those in uncovered films. However, it is remarkable that the diffraction efficiencies are as high as or even higher than the case of uncovered films. While the surface relief is suppressed, the anisotropy seems to have increased in these films, as expected from their larger local density.

AFM scanning has also been undertaken on **PC6Mn-(2)**, **PC8Mn(1)**, **PC8Mn(2)**, and **PC8Mn(3)** films after they have been irradiated through a transmission mask. The mask consists of a periodic amplitude grating, with a period of 30 μm with the width of the transparent region being 5 μm. The film was placed on the grating and was irradiated with polarized light. On irradiation with light polarized perpendicular to grating lines, trenches were found to appear in the irradiated area, for large fluences, confirming the observations made earlier in the diffraction measurements.

4. Conclusion

Side-chain azobenzene polymers having a polymethacrylate main chain have been synthesized and examined for optical storage. After irradiation at 488 nm with a polarized laser beam, these materials present a fairly large diffraction efficiency that is stable at room temperature. As in other azobenzene-containing systems, a strong surface relief was observed in the area irradiated with two orthogonally circularly polarized beams. Remarkably, not the homopolymers but polymers with 75−80% dye content exhibit the largest surface relief. The effect of the chirality of the side chains is, however, not clear. More experiments with chiral and nonchiral side groups are necessary to evaluate their contribution.

Acknowledgment. L.A. (University of Pisa) and S.H. and P.S.R. (Risø National Laboratory) gratefully acknowledge the financial support for this research from the Danish Polymer Centre supported by the Danish Materials Technology Development Program (MUP2). Dan Disc A/S is thanked for the loan of the Dektak 3030 surface profile system.

References and Notes

(1) Ringsdorf, H.; Schmidt, H. W. *Makromol. Chem*. **1984**, *185*, 1327.
(2) Eich, M.; Wendorff, J. H. *J. Opt. Soc. Am. B* **1990**, *7*, 1428.
(3) Xie. S.; Natansohn, A.; Rochon, P. *Chem. Mater.* **1993**, *5*, 403.
(4) Hvilsted, S.; Andruzzi, F.; Kulinna, C.; Siesler, H. W.; Ramanujam, P. S. *Macromolecules* **1995**, *28*, 2172.
(5) Berg, R. H.; Hvilsted, S.; Ramanujam, P. S. *Nature* **1996**, *383*, 505.
(6) Brown, D.; Natansohn, A.; Rochon, P. *Macromolecules* **1995**, *28*, 6116.
(7) Ho, M. S.; Natansohn, A.; Rochon, P. *Macromolecules* **1996**, *29*, 44.

(8) Ho, M. S.; Natansohn, A.; Barrett, C.; Rochon, P. *Can. J. Chem.* **1995**, *73*, 1773.
(9) Natansohn, A.; Rochon, P.; Pezolét, M.; Buffeteau, T.; Ming, X. *Proc. SPIE* **1997**, *2998*, 185.
(10) Altomare, A.; Ciardelli, F.; Lima, R.; Solaro, R. *Chirality* **1991**, *3*, 292.
(11) Ciardelli, F.; Altomare, A.; Solaro, R.; Carlini, A.; Angiolini, L. *Indian J. Technol.* **1993**, *31*, 278.
(12) Altomare, A.; Ciardelli, F.; Ghiloni, M. S.; Solaro, R. *Gazz. Chim. Ital.* **1997**, *127*, 143.
(13) Altomare, A.; Ciardelli, F.; Ghiloni, M. S.; Solaro, R.; Tirelli, N. *Macromol. Chem. Phys.* **1997**, *198*, 1739.
(14) Ciardelli, F.; Carlini, C.; Solaro, R.; Altomare, R.; Pieroni, O.; Houben, J. L.; Fissi, A. *Pure Appl. Chem.* **1984**, *56*, 329.
(15) Ciardelli, F.; Pieroni, O.; Fissi, A.; Altomare, A.; Solaro, R.; Tirelli, N. *Polym. Adv. Technol.* **1995**, *6*, 32.
(16) Altomare, A.; Solaro, R.; Angiolini, L.; Caretti, D.; Carlini, C. *Polymer* **1995**, *36*, 3819.
(17) Rochon, P.; Batalla, E.; Natansohn, A. *Appl. Phys. Lett.* **1995**, *66*, 136.
(18) Kim, D. Y.; Tripathy, S. K.; Li, L.; Kumar, J. *Appl. Phys. Lett.* **1995**, *66*, 1166.
(19) Kim, D. Y.; Li, L.; Jiang, X. L.; Shivashankar, V.; Kumar, J.; Tripathy, S. K. *Macromolecules* **1995**, *28*, 8835.
(20) Barrett, C. J.; Natansohn, A. L.; Rochon, P. L. *J. Phys. Chem.* **1996**, *100*, 8836.
(21) Ramanujam, P. S.; Holme, N. C. R.; Hvilsted, S. *Appl. Phys. Lett.* **1996**, *68*, 1329.
(22) Altomare, A.; Andruzzi, L.; Ciardelli, F.; Gallot, B.; Solaro, R. *Polym. Int.*, in press.
(23) McArdle, C. B., Ed. *Side Chain Liquid Crystalline Polymers;* Blackie and Son Ltd.: Glasgow, UK, 1989; p 143.
(24) Natansohn, A.; Rochon, P.; Pézolet, M.; Audet, P.; Brown, D.; To, S. *Macromolecules* **1994**, *27*, 2580.
(25) Bartholomeusz, B. J. *Appl. Opt.* **1992**, *31*, 909.
(26) Holme, N. C. R.; Nikolova, L.; Ramanujam, P. S.; Hvilsted, S. *Appl. Phys. Lett.* **1997**, *70*, 1518.
(27) Pedersen, T. G.; Johansen, P. M.; Holme, N. C. R.; Ramanujam, P. S.; Hvilsted, S. *Phys. Rev. Lett.* **1998**, *80*, 89.
(28) Archut, A.; Vogtle, F.; De Cola, L.; Azzelini, G. C.; Balzani, V.; Ramanujam, P. S.; Berg, R. H. *Chem.-Eur. J.* **1998**, *4*, 699.
(29) Ramanujam, P. S.; Holme, N. C. R.; Nikolova, L.; Berg, R. H.; Hvilsted, S.; Kristensen, E. T.; Kulinna, C.; Nielsen, A. B.; Pedersen, M. *Proc. SPIE* **1997**, *3011*, 319.

MA980160J